Research Results in Pharmacology

Research Results in Pharmacology 8(1): 1–11
UDC: 54.057, 547.831.8, 616.8-009.7
DOI 10.3897/rrpharmacology.8.80504

Research Article

Synthesis, molecular docking, ADMET study and in vitro pharmacological research of 7-(2-chlorophenyl)-4-(4-methylthiazol-5-yl)-4,6,7,8-tetrahydroquinoline-2,5(1H,3H)-dione as a promising non-opioid analgesic drug

Aleksey D. Kravchenko[1], Natalia V. Pyatigorskaya[1], Galina E. Brkich[1], Larysa V. Yevsieieva[2], Alexander V. Kyrychenko[2], Sergiy M. Kovalenko[1,2]

1 *I.M. Sechenov First Moscow State Medical University (Sechenov University), 8 Trubetskaya St., Moscow 119991, Russia*

2 *V.N. Karazin Kharkiv National University, 4 Svobody Sq., Kharkiv 61022, Ukraine*

Corresponding author: Aleksey D. Kravchenko (aleksej_kravchenko97@mail.ru)

Academic editor: Mikhail Korokin ♦ **Received** 13 December 2021 ♦ **Accepted** 5 February 2022 ♦ **Published** 16 February 2022

Citation: Kravchenko AD, Pyatigorskaya NV, Brkich GE, Yevsieieva LV, Kyrychenko AV, Kovalenko SM (2022) Synthesis, molecular docking, ADMET study and in vitro pharmacological research of 7-(2-chlorophenyl)-4-(4-methylthiazol-5-yl)-4,6,7,8-tetrahydroquinoline-2,5(1H,3H)-dione as a promising non-opioid analgesic drug. Research Results in Pharmacology 8(1): 1–11. https://doi.org/10.3897/rrpharmacology.8.80504

Abstract

Introduction: The discovery of novel drugs that can block the transmission of pain signals for treating the pain of various etiologies is an urgent topic in pharmaceutics. The aim of this paper is to synthesize and to investigate *in vitro* and *in silico* characteristics of a promising novel compound: 7-(2-chlorophenyl)-4-(4-methylthiazol-5-yl)-4,6,7,8-tetrahydroquinoline-2,5(1H,3H)-dione (HSV-DKH-0450).

Materials and methods: The specific activity and the inhibitory mechanism of HSV-DKH-0450 were studied using the HEK293 culture cells expressing the IPTG-induced TRPA1 ion channels. Cardiotoxicity was determined by estimating the binding of HSV-DKH-0450 to the hERG channel. Inhibition of human liver cytochromes was determined by the effect on the activity of cytochromes 1A2, 2C9, 2D6, 2C8, and 3A4. Cellular toxicity was assessed by the effect on the viability of human hepatocytes. ADMET properties were evaluated using admetSAR and SwissADME web-based tools. Molecular docking was carried out using AutoDock Vina tools to predict the binding affinity of all HSV-DKH-0450 stereoisomers toward the TRPA1 and TRPV1 receptors.

Results and discussion: *In silico* predictions of ADMET properties of HSV-DKH-0450 showed that it has optimal pharmaceutical profiles. A series of *in vitro* pharmacological studies revealed that HSV-DKH-0450 is a promising antagonist of the TRPA1 ion channel with the IC_{50} of 91.3 nM. The molecular docking of HSV-DKH-0450 stereoisomers against the TRPA1 and TRPV1 receptors demonstrates that they all are characterized by an approximately similar high binding affinity.

Conclusion: The obtained data for substance HSV-DKH-0450 look promising for its further development as a potential therapeutic agent for pain relief.

Copyright *Kravchenko AD et al.* This is an open access article distributed under the terms of the Creative Commons Attribution License (CC-BY 4.0), which permits unrestricted use, distribution, and reproduction in any medium, provided the original author and source are credited.

Graphical abstract:

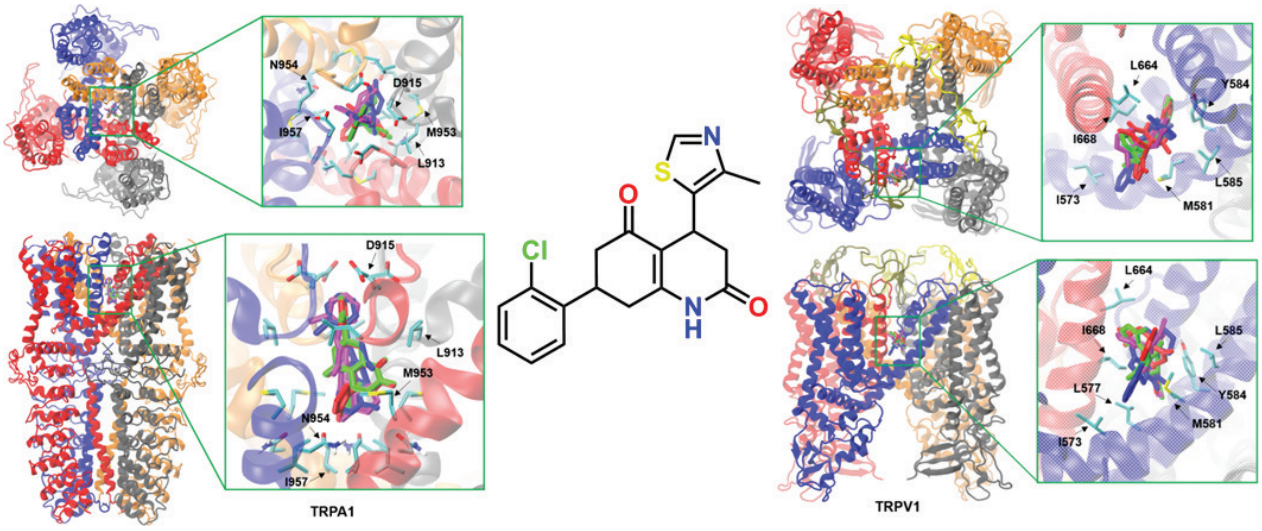

Keywords

antagonist, drug discovery, ion channels, molecular docking, TRPA1, TRPV1.

Introduction

Transient receptor potential (TRP) ion channels play a crucial role in somatic sensitivity, acting as sensors for thermal and chemical stimuli and in the formation and maintenance of inflammation. These ion channels are formed by channel-forming proteins – integral membrane proteins that ensure the transport of ions across the lipid membrane. A TRP family is organized by six loops of such transmembrane proteins that penetrate across the cell membrane and assemble into channels, which are most permeable to Ca^{2+} ions (Kamchatnov et al. 2014). Therefore, TRP ion channels activation of the cell membrane serves as an essential entry pathway of Ca^{2+} ions that also contribute to the fluctuations of intracellular concentration of Ca^{2+} and the corresponding cell signaling pathways (Yin et al. 2018).

The transient receptor potential ankyrin 1 (TRPA1) is a Ca^{2+} permeable cation channel, which is implicated in many sensory disorders, such as pain, pruritus, and neuropathy, respectively. TRPA1 activation is associated with sensitivity to chemical, electrical, and thermal stimuli (Wang et al. 2008). Another ion channel, related to TRPA1, is the transient receptor potential vanilloid subtype 1 (TRPV1), which is associated with the transmission of pain signals upon neuropathic pain. TRPV1 ion channel is activated by external factors, including such stimuli as high temperature and chemical irritation (Hasan et al. 2017). It has been found that inflammatory mediators bind to the receptors and initiate a signaling cascade that finally leads to an influx of Ca^{2+} ions. This influx is partially mediated by the opening of the Ca^{2+} ion-permeable TRPA1 and TRPV1 channels. Ca^{2+} is a secondary messenger that plays a crucial role in the TRPA1 regulation. This mechanism also underlies the indirect TRPA1 activation by inflammatory mediators, acting by increasing the influx of Ca^{2+} ions.

TRPA1 and TRPV1 activation can, in turn, induce neurogenic inflammation, which has been studied in the respiratory tract, following the release of inflammatory neuropeptides. Such positive feedback contributes to the intensification of the inflammatory process and, therefore, is related to self-sustaining neurogenic inflammation (Xu et al. 2019). TRPA1 and TRPV1 play a vital role in the occurrence of various physiological processes and pathological conditions, such as chemoreception, pain, pruritus, inflammation, neuropathy, and respiratory diseases. Therefore, these receptors are often considered to be promising targets for the molecular design of novel biologically active molecules that can inhibit the ion channel, offering opportunities for the development of promising analgesic and other therapeutic agents (Paulsen et al. 2019).

As a result of the studies (Beskhmelnitsyna et al. 2015), focused on the screening and discovering new substances capable of pain relief, we have identified a new promising compound HSV-DKH-0450 with TRPA1 antagonist activity (Fig. 1).

The HSV-DKH-0450 structure contains two chiral centers, so that it can exist as four stereoisomers (two pairs of enantiomers: RS and SR, RR and SS), as shown in Fig. 2.

In this paper, we estimated the ADMET properties for compound HSV-DKH-0450 and found out that it has a high human intestinal absorption rate, so it can be administered orally. *In vitro* studies demonstrated that HSV-DKH-0450

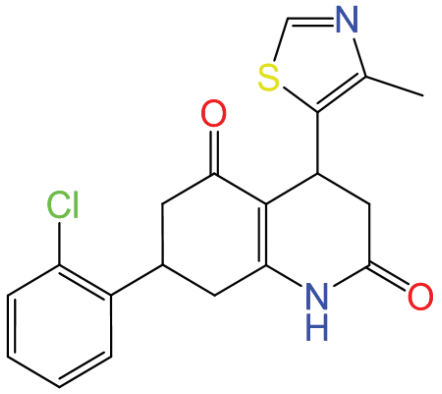

Figure 1. The chemical structure of 7-(2-chlorophenyl)-4-(4-methylthiazol-5-yl)-4,6,7,8-tetrahydroquinoline-2,5(1H, 3H)-dione (HSV-DKH-0450).

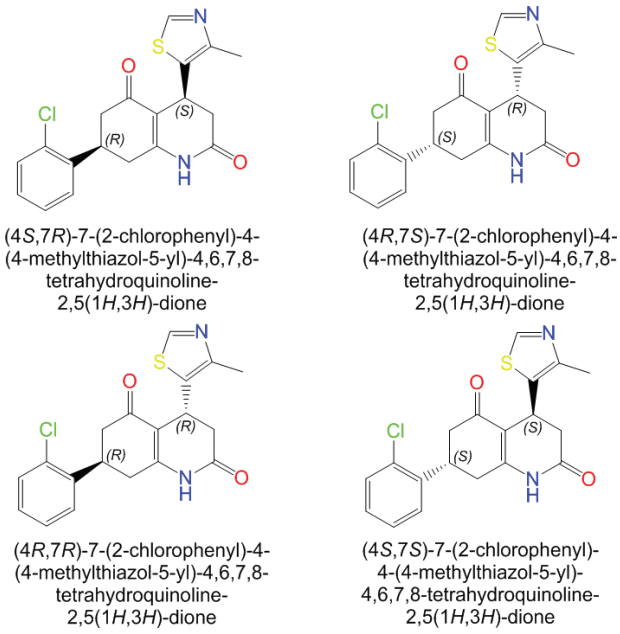

Figure 2. Structures of four possible HSV-DKH-045 stereoisomers.

obtained according to the procedure described below is a promising TRPA1 antagonist with IC_{50} of 91.3 nM, which is about the same level of activity as the standard control antagonist Ruthenium Red. Moreover, several lines of evidence point to a low risk of cardiotoxicity and hepatotoxicity caused by HSV-DKH-0450. Taken together, a series of *in vitro* tests allowed us to suggest the high selectivity of HSV-DKH-0450 as an inhibitor of the TRPA1. Finally, the molecular-level details of inhibitor-receptor interactions and the inhibitory mechanism of TRPA1 by HSV-DKH-0450 were studied using molecular docking calculations. The molecular docking of all possible stereoisomers of HSV-DKH-0450 towards several cryo-EM structures of the TRPA1 receptor demonstrated that they all bind within the TRPA1 ion channel pore with high docking scores. Moreover, the binding affinity of all four stereoisomers into the TRPA1 receptor is observed at a very similar level so that no essential inhibitory stereoselectivity is expected.

Materials and methods

Materials

All the chemicals were obtained from Sigma-Aldrich or Merck. ^{1}H NMR spectra were registered on a Bruker DPX 300 spectrometer (Bruker BioSpin AG, Industriestrasse 26, 8117 Fällanden, Switzerland) at room temperature (298 K) using DMSO-d6 as a solvent and processed using Bruker XWinNMR software (International Equipment Trading Ltd., Mestrenova Version 9.0 Spain, Vernon Hills, IL 60061, USA).

Synthesis

HSV-DKH-0450 was synthesized by the following three-stage procedure (Fig. 3) as described below:

Synthesis of 7-(2-chlorophenyl)-4-(4-methylthiazol-5-yl)-4,6,7,8-tetrahydroquinoline-2,5(1H,3H)-dione (HSV-DKH-0450)

Stage 1. ***2,2-Dimethyl-5-[(4-methyl-1,3-thiazol-5-yl) methylene]-1,3-dioxane-4,6-dione***

4-methyl-1,3-thiazole-5-carbaldehyde (148 g) and 2,2-dimethyl-1,3-dioxane-4,6-dione (167 g, 1 equiv.) were added to 1.5 L of ethyl alcohol. Upon stirring the reaction mixture, dimethylaminopyridine (14 g, 0.1 equiv.) was added as a catalyst. The reaction mass was stirred at 22 °C (room temperature) for 48 hours. While stirring the reaction mixture, the precipitate partially dissolved and then reprecipitated. A sample of the reaction mass was analyzed by the ^{1}H NMR method. The sample spectrum should contain no proton signals corresponding to the original 4-methyl-1,3-thiazole-5-carbaldehyde. A suspension of the reaction product and the catalyst in ethyl alcohol was filtered under vacuum. The precipitate was carefully squeezed out and laid out on a cuvette to dry in the air at room temperature for 10 hours. 2,2-dimethyl-5-[(4-methyl-1,3-thiazol-5-yl)methylene]-1,3-dioxane-4,6-dione (250±3 g) was obtained as bright yellow powder. The reaction yield was 85–86%. The sample was characterized by the following peaks: ^{1}H NMR (400 MHz, DMSO-D6) δ ppm 1.7 (s, 6 H), 2.7 (s, 3 H), 8.6 (s, 1 H), 9.5 (s, 1 H), respectively.

Stage 2. ***3-[4-(2-Chlorophenyl)-2-hydroxy-6-oxocyclohex-1-en-1-yl]-3-(4-methyl-1,3-thiazol-5-yl)propanoate***

2,2-dimethyl-5-[(4-methyl-1,3-thiazol-5-yl)methylene]-1,3-dioxane-4,6- dione (250 g) and 5-(2-chlorophenyl)-3-hydroxycyclohex-2-en-1-one (220 g, 1 equiv.) were added to 1.5 L of ethyl alcohol. 1,4-diazobicyclooctane (6 g, 0.05 equiv.) was added as a catalyst, while stirring. The reaction mass was stirred for 24 hours at room temperature, while the precipitate partially dissolved and fell out again, then the mixture thickened so much that it ceased to stir, and the reaction mass was kept for another 24 hours at room temperature. The reaction mass

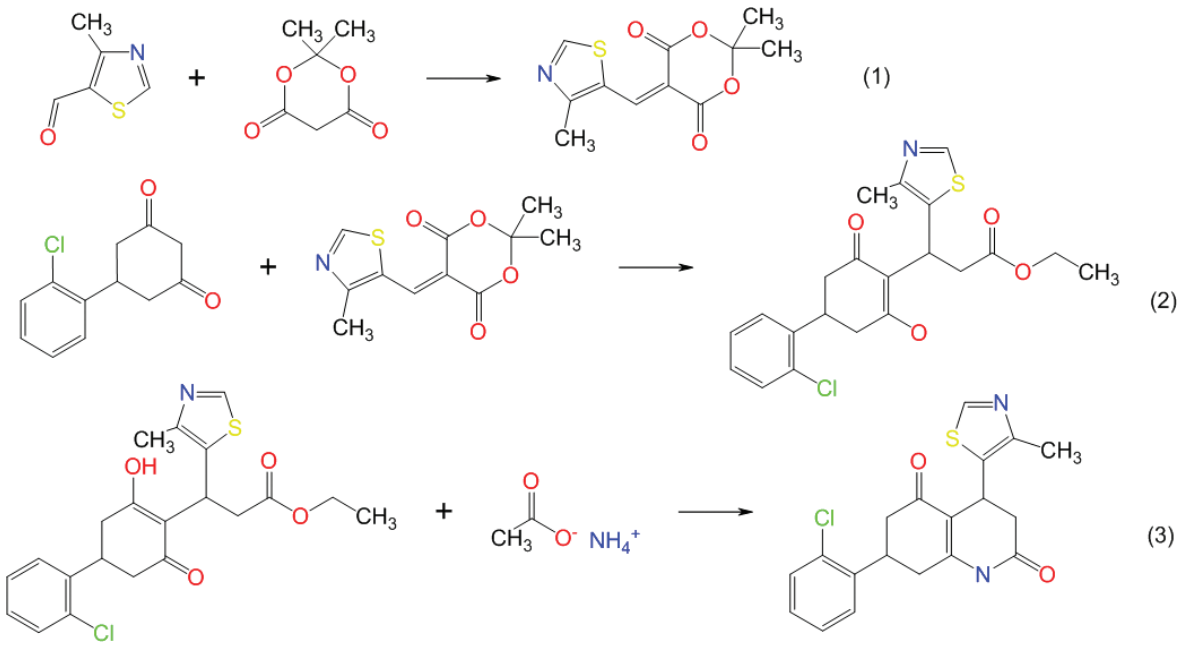

Figure 3. Scheme of HSV-DKH-045 synthesis.

sample was analyzed by the ^{1}H NMR spectroscopy. The spectrum of the sample should contain no proton signals corresponding to the initial 2,2-dimethyl-5-[(4-methyl-1,3-thiazol-5-yl)methylene]-1,3-dioxane-4,6-dione. An ethanol suspension of the reaction product and the catalyst was then filtered under vacuum. The obtained precipitate was washed with diethyl ether (500 ml). The precipitate was carefully squeezed out and laid out on a cuvette to dry in the air at room temperature for 10 hours to give 3-[4-(2-chlorophenyl)-2-hydroxy-6-oxocyclohex-1-en-1-yl]-3-(4-methyl-1,3-thiazol-5-yl)propanoate (282±3 g) as white powder. The reaction yield was 68–69%. The product was characterized by the following spectral peaks: ^{1}H NMR (300 MHz, DMSO-D6) δ ppm 1.1 (t, J = 7.1 Hz, 4 H), 2.4 (s, 4 H), 2.5 (s, 2 H), 2.7 (s, 2 H), 2.9 (dd, J = 15.4, 6.8 Hz, 1 H), 3.1 (m, 2 H), 3.6 (s, 1 H), 4.0 (m, J = 7.1, 7.1, 6.9, 1.9 Hz, 2 H), 5.0 (m, 1 H), 7.3 (m, J = 7.3, 7.0, 6.9, 6.9, 1.8 Hz, 2 H), 7.4 (d, J = 7.6 Hz, 2 H) 8.7 (s, 1 H).

Stage 3. *7-(2-chlorophenyl)-4-(4-methyl-1,3-thiazol-5-yl)-4,6,7,8-tetrahydroquinoline-2,5 (1H, 3H)-dione (HSV-DKH-0450)*

Ammonium acetate (1034 g, 20 equiv.) and acetic acid (850 ml) were mixed in a beaker. The mixture was stirred and heated to reflux (118 °C), with the temperature control of the magnetic stirrer set at 150 °C. After that, 3-[4-(2-chlorophenyl)-2-hydroxy-6-oxocyclohex-1-en-1-yl]-3-(4-methyl-1,3-thiazol-5-yl)propanoate (282 g) was added step-by-step, and the mixture continued to boil for another 1.5 hours. The reaction mass was monitored by TLC using chloroform-methanol 10:1 as eluent. As purity control, there should be no peaks corresponding to the initial reagents on the chromatogram of the reaction mass. After the reaction was finished, the heating was turned off and the mixture was kept at 22 °C for 48 hours. The precipitate was filtered under vacuum and washed with methyl tertiary-butyl ether (850 ml) and squeezed thoroughly. The precipitate was placed in a beaker without drying, and chloroform (850 ml) was added to the precipitate. After the dissolution, the product solution in chloroform was transferred into a separatory funnel and successively washed with water (850 ml), then with potassium carbonate solution (5%, 850 ml), prepared by dissolving potassium carbonate (45 g) in water (830 ml). Next, the chloroform layer was dried with sodium sulfate (141 g). Silica gel (282 g) was placed on a Schott filter and tamped. The product solution in chloroform was carefully poured onto a layer of silica gel and allowed to drain by gravity into a conical flask, after which the silica gel was washed with 2 L of chloroform. The combined chloroform solution was transferred in portions from the conical flask to the rotary evaporator flask to remove the solvent. The filtrate was added in portions to the flask as the solvent was removed, the solvent was removed at 40 °C (bath temperature) until light brown dry foam was formed. The residue was cooled down to 22 °C and methyl tertiary-butyl ether (3.1 L) was poured into a conical flask. The mixture was stirred and heated up to boiling (55 °C), with the temperature control of the magnetic stirrer set at 75 °C. The solution was kept under these conditions for 24 hours. After that, the solution was cooled down to 22 °C and filtered under vacuum. The sediment of the substance (HSV-DKH-045) was transferred to a drying tray and dried in a vacuum drying oven at a residual pressure of not more than 20 mm Hg at 30 °C for 12 hours to give the final compound HSV-DKH-045 (180±0.3 g) as white powder. The reaction yield was 72–73%. The product was characterized by the following spectral peaks: ^{1}H NMR (300 MHz, DMSO-D6) δ ppm 2.35–2.47 (m, 5 H), 2.60–3.10 (m, 4 H), 3.60–3.90 (m, 1 H), 4.47–4.55 (m, 1 H), 7.25- 7.60 (m, 4 H), 8.71–8.77 (m, 1 H), 10.40–10.50 (m, 1 H).

ADMET study

The ADMET properties of a compound characterize its Absorption, Distribution, Metabolism, Excretion, and Toxicity in the human body. The ADMET parameters help predict and evaluate the pharmacokinetic profile of a molecule as an active pharmaceutical ingredient candidate. In this study, we used the web-based forecasting tools for evaluating ADMET properties – admetSAR (Cheng et al. 2012) and SwissADME (login-free website http://www.swissadme.ch).

Pharmacological research

The study of the specific activity and the inhibitory mechanism of compound HSV-DKH-0450 was carried out *in vitro* using a HEK293 cell culture (human embryonic epithelial cells of the human kidney), exogenously expressing IPTG (isopropyl-β-D-1-thiogalactopyranoside)-inducible TRPA1 ion channel. The TRPA1 ion channel activity was stimulated by the agonist AITC (allylisothiocyanate), which activated the release of Ca^{2+} ions into the cell cytoplasm. The inhibitory activity of HSV-DKH-0450 was measured by a decrease in the Ca^{2+} concentration in the cell cytoplasm, using a Fluorescent Imaging Plate Reader (FLIPR). Ruthenium Red (RR) was used as a standard control antagonist for the TRPA1 ion channel.

Culture medium: DMEM mixture (Hyclone, USA), 10% FBS (Hyclone, USA), 1% NEAA, Sodium pyruvate, 2 mM L-glutamine, 0.3 µg/ml G418, 20 µg/ml hygromycin. Subcultured cells ready for the experiment were suspended in a culture medium with 1mM IPTG so that a cell concentration was $8 \cdot 10^5$ cells/ml. The cells were transferred to 384-well experimental culture plates, with an optical bottom using automatic robotic stations Biomek FX or Biomek NX, using 25 µl of suspension per well (20,000 cells per well). After that, the plates were centrifuged for 5 minutes at 200 g and incubated for 24 hours at 37 °C in the presence of 5% CO_2. A fluorescent indicator sensitive to changes in intracellular calcium FLIPR Calcium 4 Assay Kit (Hansen and Bräuner-Osborne 2009) was used to determine the specific activity. On the day of the experiment, the cells were mixed with a Ca^{2+}-sensitive indicator, incubated for 1 hour at room temperature in a dark place, and started reading on the FLIPR.

Serial dilution with a step of 3.16, carried out with the Biomek 2000, starting with an initial 10 mM solution of the test substance in DMSO was used to study the antagonistic activity. At a 166.6-fold dilution in a mixture of HHBS buffer (Hanks' Balanced Salt Solution with 20 mM Hepes buffer)/0.6% Pluronic F127 (PF-127)/0.6% DMSO, a 6-fold stock solution of a batch of substances was obtained. The final maximum tested concentration was 30 µM. Stimulation of the TRPA1 ion channel was performed using an EC_{80} agonist AITC with a concentration of 30 µM. To inhibit the stimulated Ca^{2+} response, the maximum inhibitory concentration of the control antagonist IC_{100} equal to 6 µM was used. 12.5 µl of substance was added to each well of the 384-well plate according to the plate design to detect the activity of the tested substances. After that, the experimental plate was analyzed by a FLIPR reader. After incubation for 11 minutes, 12.5 µl of an AITC agonist was added to each well of the 384-well experimental plate and a second measurement by the FLIPR reader was immediately initiated to determine antagonists. The IC_{50} value for antagonists was calculated using the obtained dependence of antagonist activity on concentration (GraphPad Prizm software, GraphPad Software, Inc., San Diego, CA).

The cellular toxicity of the test compound was assessed by the effect of the *in vitro* survival of human hepatocytes. The study was carried out on cryo-frozen hepatocytes during their incubation with the inhibitor for 24 h stored in a CO_2 incubator, using 4 wells for each concentration. The final cell concentration was 10,600 cells/well. The range of investigated concentrations of HSV-DKH-04500 was 0.0032–31.6 µM. The number of living cells was assessed using the CellTiter-Glo test system (Promega). Tubercidin was used as a cytotoxic control compound.

A safety study was also evaluated for inhibition of human liver cytochromes. The effect of HSV-DKH-0450 on the activity of isoforms 1A2, 2C9, 2C19, 2D6, 2C8, and 3A4 of cytochrome P450 (CYP450) in human liver microsomes was determined using metabolic substrates specific for the corresponding cytochrome isoenzymes. The test substances were incubated with human microsomes in the presence of NADPH and a mixture of 7 substrates in 96-well plates (substrates: phenacetin, midazolam, testosterone, tolbutamide, S-mephenytoin, dextromethorphan, amodiaquine). The reaction was stopped after 20 min by the addition of acetonitrile. The resulting metabolites were detected using HPLC-MS/MS analysis.

The IC_{50} values were determined for cytochromes 1A2, 2C9, 2C8, 2C19, 2D6, 2C8, and 3A4, respectively. Some specific inhibitors, such as α-naphthoflavone, sulfafenozole, fluvoxamine, quinidine, quercetin, and ketoconazole, were used as controls. The final concentration range of compound HSV-DKH-04500 was 10.0–0.0098 µM. To calculate the concentration of metabolites, we used calibration curves constructed from the values of the chromatographic peak areas normalized to the signal of the internal standard.

The HSV-DKH-0450 binding to the hERG-voltage-dependent K^+ ion channel of cardiomyocytes was studied using the *in vitro* test system Invitrogen PredictorTM hERG. A membrane fraction containing the hERG channel protein (Predictor hERG Membrane), which has a high affinity for the red fluorescent ligand of the hERG channel, the tracer (Predictor hERG Tracer Red), was used for the analysis. The method is based on the detection of changing fluorescence polarization, which decreases when a high-affinity fluorescent ligand – tracer is displaced by the test substance. Binding measurement was carried out at eight concentrations of the test substance in the range of 0.014–30.0 µM, respectively. The study of the HSV-DKH-0450 selectivity was carried out using a

panel of 80 receptors and their specific ligands. Inhibition of specific binding of ligands by 50% or more was considered significant. The study was carried out at an HSV-DKH-0450 concentration of 10 μM.

Molecular docking

AutoDock Vina 1.1.2 software was used to perform the Molecular docking calculations (Trott et al. 2010). During the docking, the receptor was kept rigid, and the ligand molecules were conformationally flexible. The Lamarckian genetic algorithm was used as a research parameter. The size of the cubic box generated by ADT in the region of the TRPA1 and TRPV1 receptors was defined as 100×100×100 Å. The grid point spacing was set to 0.375 Å. The number of ligand binding modes was set to 9 and the Vina exhaustiveness parameter – to 64. For each ligand, three independent searches were performed using different random seeds. The best docking mode corresponds to the largest ligand-binding affinity. VMD 1.9.3 was used to perform the molecular graphics and visualization (Humphrey et al. 1996).

Results and discussion

The ADMET properties for HSV-DKH-0450 were calculated by the AdmetSAR and SwissADME servers. The results suggest that HSV-DKH-0450 has a high human intestinal absorption rate (HIA). It means that compound HSV-DKH-0450 can be well absorbed from the intestinal tract when administered orally. In addition, compound HSV-DKH-0450 is a substrate for glycoprotein P, so that it will be easily excreted from the body without accumulating. Moreover, several lines of evidence suggest that HSV-DKH-0450 meets the optimal pharmacokinetic parameters and obeys the Lipinski rule for drug-like molecules used as active pharmaceutical ingredients. The Lipinski rule suggests that drug-like molecule should fall within the following ADMET parameters: logP: -0.7 to +5.0, M_W: 150 to 500 g/mol, polar surface area: TPSA from 20 to 130 Å^2, solubility: logS not more than 6; saturation: carbon atoms in sp^3 hybridization not less than 0.25; flexibility: not more than 9 rotating bonds, respectively.

To confirm that HSV-DKH-0450 is a promising antagonist of the TRPA1 ion channel, we carried out *in vitro* studies. The IC_{50} for HSV-DKH-0450 was found to be 91.3 nM. This value was a little less than the IC_{50} for Ruthenium Red – the standard control antagonist for the TRPA1 ion channel with IC_{50} = 118.2 nM. Next, predicting possible hepatotoxicity is an essential step in drug safety studies. Our studies have shown that HSV-DKH-0450 does not affect the viability of hepatocytes at concentrations up to 30 μM, so HSV-DKH-0450 is not hepatotoxic. To determine the possible cardiotoxic effect for the compound HSV-DKH-0450, binding to the hERG channel was also evaluated. The test compound HSV-DKH-0450 was determined to have no essential effect on hERG at all tested concentrations up to 30 μM. These data suggest a low risk of HSV-DKH-0450 cardiotoxicity.

To examine the inhibitory affinity of HSV-DKH-0450 for suppressing the activity of isoforms 1A2, 2C9, 2C19, 2D6, 2C8, and 3A4 of cytochrome P450 (CYP450) in human liver microsomes, we used metabolic substrates, which are specific for the corresponding cytochrome isoenzymes. It was determined that the test compound does not reveal an essential inhibitory effect on the activity of cytochromes 1A2, 2C9, 2D6, 2C8, and 3A4, so that IC_{50} estimated to be > 10 μM. In addition, weak inhibition of 2C19 isoenzyme by HSV-DKH-0450 is observed with IC_{50} = 3.4 μM.

A study of the selectivity of HSV-DKH-0450 on a panel of enzymes and receptors showed that HSV-DKH-0450 is characterized by high selectivity so that on a panel of 80 targets, the substance showed significant binding only towards the melatonin MT1 receptor and the dopamine transporter. Taking into account that the study was carried out at a concentration of HSV-DKH-0450 of 10 μM, and the activity of this compound on the studied target TRPA1 is almost 100 times higher (IC_{50} ~ 100 nM), we can suggest the high selectivity of HSV-DKH-0450 as an inhibitor of the ionic TRPA1 channel.

To study molecular aspects of binding affinity of HSV-DKH-0450 to TRPA1 receptor, we carried out a series of molecular docking calculations. First, we analyzed

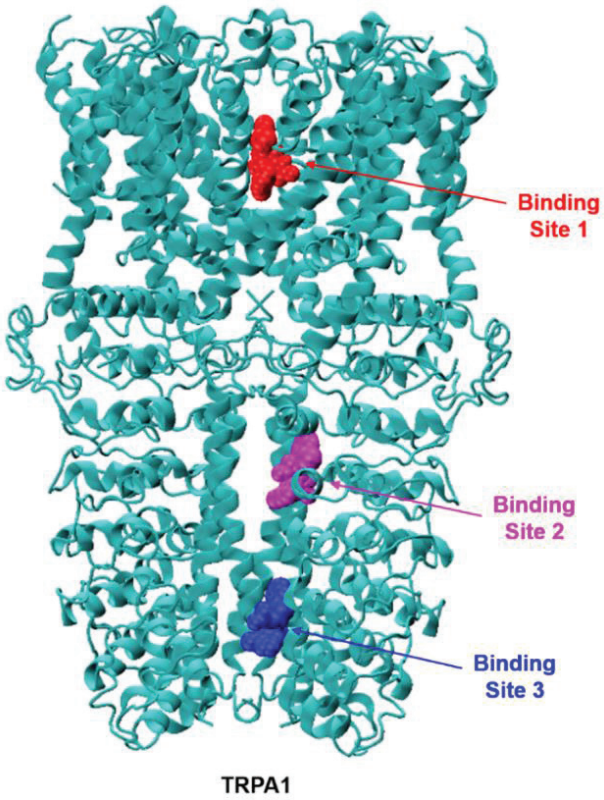

Figure 4. The three most stable binding sites of (4R, 7R)-HSV-DKH-0450 stereoisomer at TRPA1 ion channel (PDB ID: 3J9P) identified by molecular docking calculations. Binding energies: Site 1 -8.4 kcal/mol; Site 2 -8.1 kcal/mol; Site 3 -8.0 kcal/mol, respectively.

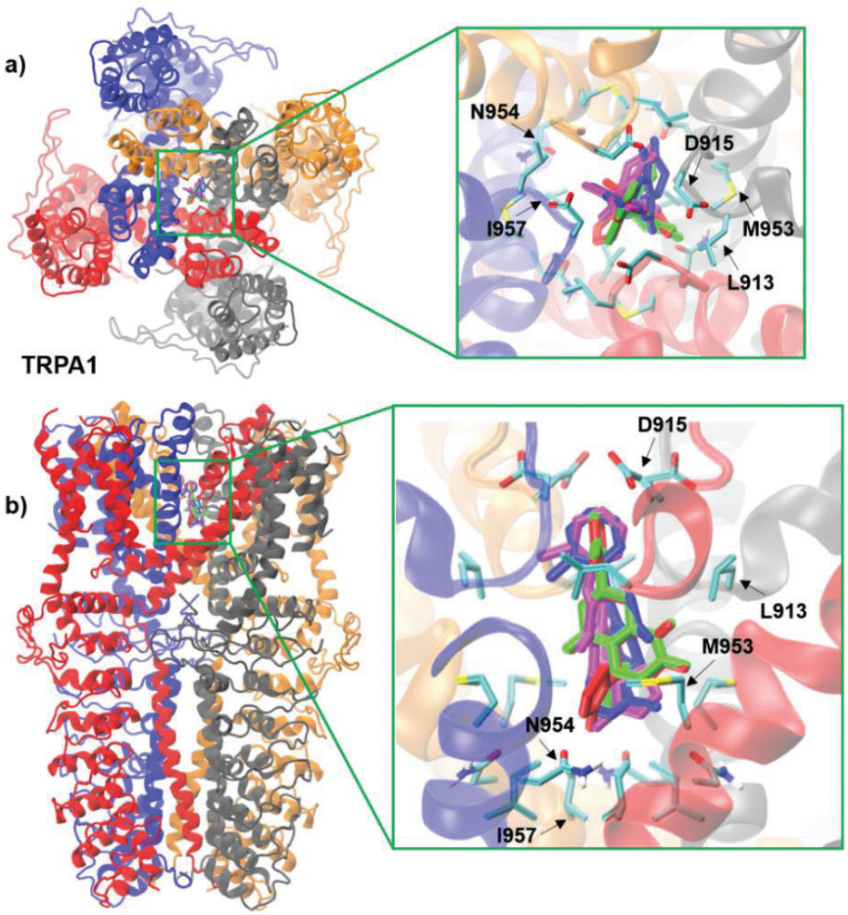

Figure 5. The best docking poses for four HSV-DKH-0450 stereoisomers at TRPA1 receptor (PDB ID: 3J9P). The protein crystal structure is shown as ribbons in the top (**a**) and the side (**b**) views and color-coded by chain A-D. The HSV-DKH-0450 ligand molecules are shown as sticks, color-coded as follows: (4R, 7R)-isomer – *red*; (4R, 7S)-isomer – *green*; (4S, 7R)-isomer – *magenta*; (4S, 7S)-isomer – *blue*.

the structure and possible binding modes of an isolated TRPA1 receptor. The TRPA1 channel is a tetrameric receptor that contains 14–16 N-terminal ankyrin repeat units and a single pore. The structure of the TRPA1 receptor was determined by electron cryo-microscopy (PDB 3J9P) at a 4.2 Å resolution (Paulsen et al. 2015). The TRPA1 ion channel structure is characterized by the fourfold symmetry. The TRPA1 transmembrane subunits contain six α-helices, an intracellular C-terminal domain, and an intracellular N-terminal domain (Fig. 4). Since its discovery, this TRPA1 ion channel structure has become a promising target for *in silico* screening and development of novel non-covalent antagonists and other selective small molecule inhibitors (Mihai et al. 2019, Ghosh et al. 2020).

Some earlier studies have shown that the TRPA1 ion channel might have several alternate interacting sites for the binding of covalent and non-covalent antagonists (Tseng et al. 2018; Mihai et al. 2019; Araki et al. 2020).

To identify potential binding sites at the TRPA1 ion channel, we first screened available binding pockets using molecular docking of HSV-DKH-0450 over three receptor regions: single-pore containing regions (binding site 1), a transmembrane domain (binding site 2), and an intracellular N-terminal domain (binding site 3), respectively. We have found that compound HSV-DKH-0450 favors the non-covalent binding at three receptor sites, referred to as Sites 1–3, as shown in Fig. 4. Binding site 1, which is located within a TRPA1 pore, is characterized by the highest docking scores for all studied stereoisomers of HSV-DKH-0450, so that our further study is primarily focused on identifying molecular-level details and energetics of interactions of HSV-DKH-0450 with TRPA1 channel at binding site 1 (Fig. 4).

The best docking poses of four HSV-DKH-0450 stereoisomers within the TRPA1 ion channel pore are shown in Fig. 5 at the top and side views. It can be noted that all four stereoisomers occupy the same area of space near the side chains Leu913, Asp915, Met953, Ile957, and Asn954, respectively.

Table 1 summarizes the docking scores of all HSV-DKH-0450 stereoisomers at the binding pocket of the TRPA1 ion channel. The binding energies range from -8.3 kcal/mol for 4R, 7S and 4S, 7R isomers up to -8.6 kcal/mol for 4S, 7S one, respectively. These data were taken after averaging three independent docking runs and suggest that the binding affinity of all four studied HSV-DKH-0450 stereoisomers are very similar.

Table 1. Docking Binding Energy (kcal/mol) for Four HSV-DKH-0450 Stereoisomers Toward Different Electron Microscopy Structures of TRPA1 and TRPV1 Ion Channels. The Structure Resolution is Given in Brackets. The Energy Corresponds to the Best Docking Pose of the Ligand

HSV-DKH-0450 stereoisomers	TRPA1			TRPV1	
	PDB:3J9P (4.24 Å)	PDB:6PQO (2.88 Å)	PDB:6PQP (3.06 Å)	PDB:5IRX (2.95 Å)	PDB:3J5P (3.27 Å)
(4R, 7R)	-8.4	-7.6	-8.1	-8.2	-7.8
(4R, 7S)	-8.3	-7.5	-8.0	-9.1	-8.0
(4S, 7R)	-8.3	-7.5	-8.4	-8.7	-8.3
(4S, 7S)	-8.6	-8.0	-7.9	-8.6	-8.3

Despite numerous docking studies based on the electron cryo-microscopy structure of TRPA1 ion channel deposited as PDB code 3J9P, a mechanistic understanding of ligand-receptor interactions has been claimed to have a lack of high-resolution details. Therefore, the high-resolution structure of human TRPA1 has recently been re-measured using cryo-electron (cryo-EM) microscopy of nanodisc-reconstituted ligand-free receptor and TRPA1 in complex with some covalent antagonists at 2.8 – 3.1 Å resolution (Ghosh et al. 2020).

We used the two recently reported structures of the TRPA1 ion channel, deposited as PDB codes 6PQO and 6PQP, as a target for HSV-DKH-0450 molecular docking. We found that the HSV-DKH-0450 docking results, which were carried out on these two receptors, agreed well with the docking calculations based on the lower-resolution TRPA1 structure (PDB 3J9P), as summarized in Table 1. The best docking poses of all four HSV-DKH-0450 stereoisomers were compared for two TRPA1 ion channel structures in Fig. 6. It should be noted that the docking poses of all HSV-DKH-0450 isomers calculated at 4.24 Å resolution TRPA1 structure were found at very similar positions (Fig. 5a, b). In contrast, the docking poses of HSV-DKH-0450 isomers, estimated for 2.88 Å resolution TRPA1 structure, vary significantly, as seen in Fig. 6c, d. The 4S, 7S-isomer prefers residing deeper in the channel pore. As a result, the docking score of 4S, 7S-isomer was found to be the most favorable (Table 1). Finally, we found that the docking results for the TRPA1 ion channel taken from the 3.06 Å resolution structure (PDB 6PQP) were very similar to those obtained by the 6PQO structure in terms of docking poses and binding scores (Table 1).

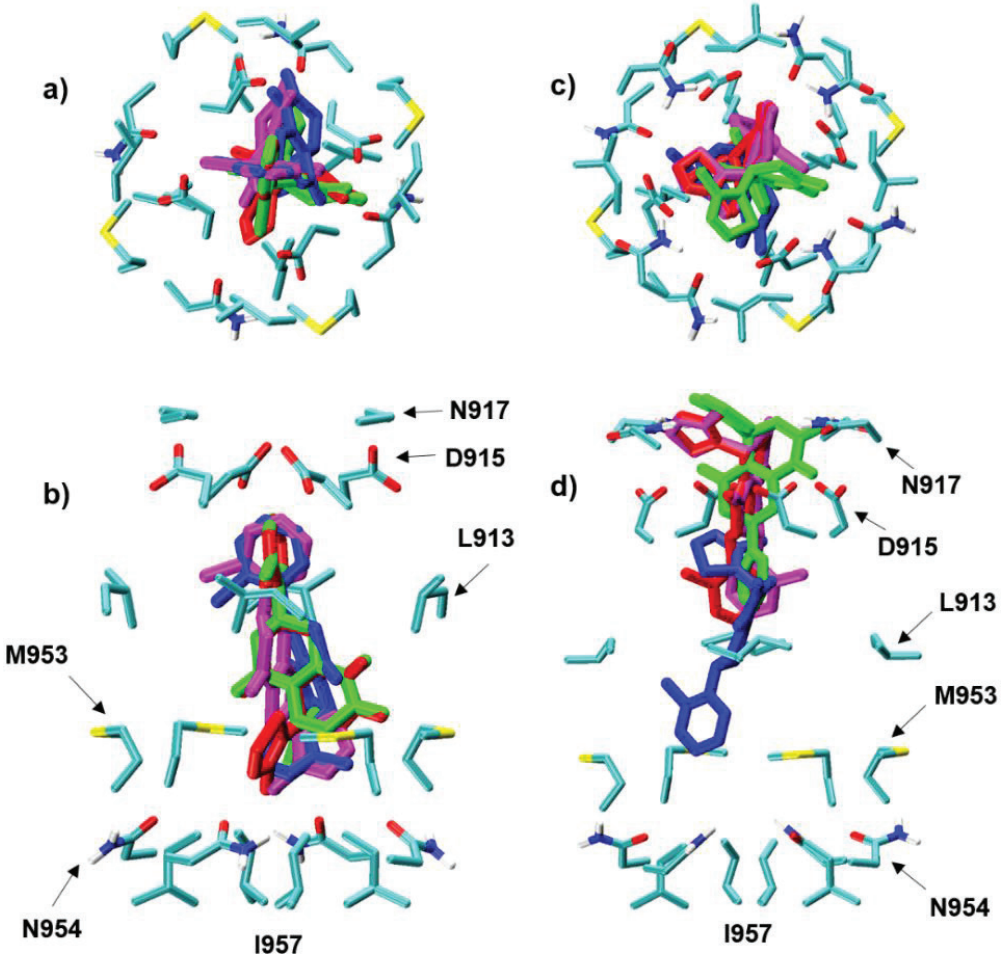

Figure 6. The comparison of the best docking poses for four HSV-DKH-0450 stereoisomers at TRPA1 ion channel taken from two different cryo-EM target structures (**a**, **b**) (PDB ID: 3J9P) and (**c**, **d**) (PDB ID: 6PQO) shown in the top (**a, c**) and the side (**b, d**) representations. The HSV-DKH-0450 ligand molecules are shown as sticks, color-coded as follows: (4R, 7R)-isomer – *red*; (4R, 7S)-isomer – *green*; (4S, 7R)-isomer – *magenta*; (4S, 7S)-isomer – *blue*.

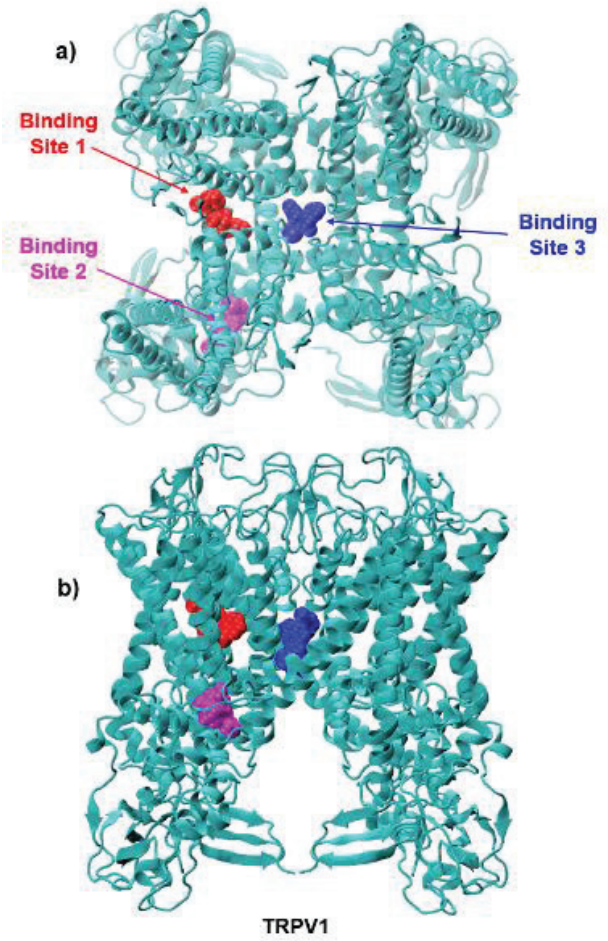

Figure 7. The three most stable binding sites of (4R, 7S)-HSV-DKH-0450 isomer at TRPV1 ion channel (PDB ID: 5IRX) identified by molecular docking calculations. Binding energies are ranked as following: Site 1: -9.1 kcal/mol; Site 2: -8.6 kcal/mol; Site 3: -8.3 kcal/mol, respectively.

The TRPA1 and TRPV1 are members of the TRP superfamily of structurally related, nonselective cation channels, which are frequently co-localized in sensory neurons and have a low threshold for various inflammatory mediators, such as bradykinins, histamines, and eicosanoids (Fernandes et al. 2012; Bousquet et al. 2021). This is why these receptors have often been considered as a common target for *in silico* design of novel TRP ion channel antagonists.

The TRPV1 ion channel Cryo-EM structure was reconstructed in a lipid nanodisc at 2.95 Å resolution (PDB 5IRX) (Gao et al. 2016). First, we identified possible binding sites of HSV-DKH-0450 antagonist at the TRPV1 ion channel by molecular docking over different receptor regions. Fig. 7 summarizes the three most favorable HSV-DKH-0450 binding sides at the TRPV1 ion channel. It should be noted that HSV-DKH-0450 prefers binding at Site 1, located in the hydrophobic pocket close to the ion channel pore (Fig. 7). Thus, the binding pocket of HSV-DKH-0450 at TRPV1 differs from its binding position observed in the TRPA1 ion channel (Fig. 4). Therefore, our further docking study was primarily focused on

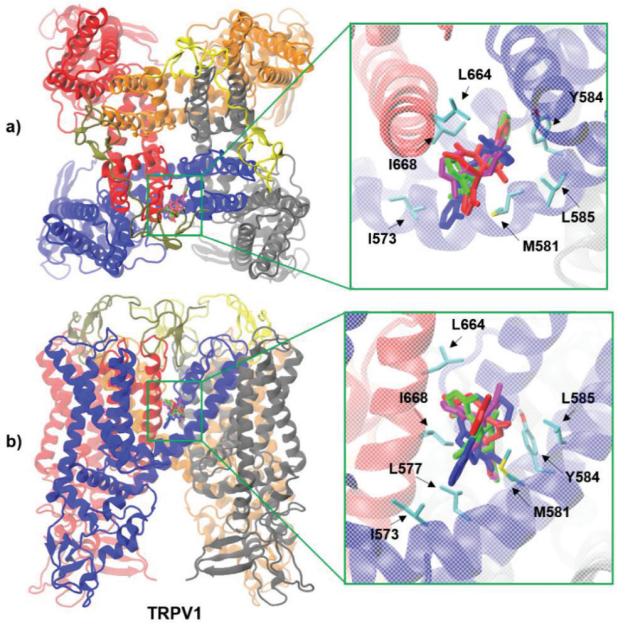

Figure 8. The best docking poses for four HSV-DKH-0450 stereoisomers at TRPV1 receptor (PDB ID: 5IRX). The protein crystal structure is shown as ribbons in the top (**a**) and the side (**b**) views and color-coded by chain A-D. The HSV-DKH-0450 ligand molecules are shown as sticks, color-coded as follows: (4R, 7R)-isomer – *red*; (4R, 7S)-isomer – *green*; (4S, 7R)-isomer – *magenta*; (4S, 7S)-isomer – *blue*.

HSV-DKH-0450 interactions with the TRPV1 channel at Binding Site 1 (Fig. 7).

Fig. 8 and Table 1 summarize the docking poses and binding scores of all HSV-DKH-0450 stereoisomers at TRPV1 Binding Site 1. The binding energies for all isomers range from -8.2 to -9.1 kcal/mol, respectively. Finally, we carried out the molecular docking of HSV-DKH-0450 against another TRPV1 cryo-EM structure (PDB 3J5P), which has often been utilized for molecular docking of other ligands (Wang et al. 2018; Benítez-Angeles et al. 2020).

Finally, the HSV-DKH-0450 molecular docking results against the TRPV1 ion channel taken from the 3.27 Å resolution structure (PDB 3J5P) are found to be very similar in many aspects to the results estimated against the high-resolution TRPV1 structure (PDB 5IRX) (Table 1).

To summarize and take into account the accuracy of the empirical scoring function used in the molecular docking calculations, we can suggest that the affinity of all four studied stereoisomers toward the TRPV1 receptor is expected to be of a very similar level.

Conclusion

A new promising antagonist HSV-DKH-0450 of the ion channels was studied using *in vitro* pharmacological tests, *in silico* screening of ADMET properties and molecular docking calculations. A series of *in vitro* pharmacological studies revealed that HSV-DKH-0450

has a high inhibitory activity against the TRPA1 ion channel with the IC_{50} of 91.3 nM. In addition, *in silico* predictions of HSV-DKH-0450 ADMET properties showed that it has pharmacokinetic and pharmacodynamics profiles that are optimal for an active pharmaceutical ingredient. The molecular docking of the four HSV-DKH-0450 stereoisomers against the TRPA1 and TRPV1 receptors demonstrates that they all are characterized by a high binding affinity. Comparison among the various isomers and the TRPA1 receptor suggests that the docking binding scores of all isomers were found to be of a similar order of magnitude, ranging from -8.3 up to -8.6 kcal/mol. Taken together, our results suggest that HSV-DKH-0450 is a promising antagonist of the TRPA1 ion channel, making it a promising chemical scaffold for further advance and developing a novel therapeutic agent for pain relief.

Funding

The authors have no funding to report.

Conflict of interest

The authors have declared that no competing interests exist.

References

- Araki M, Kanda N, Iwata H, Sagae Y, Masuda K, Okuno Y (2020) Identification of a new class of non-electrophilic TRPA1 agonists by a structure-based virtual screening approach. Bioorganic Medicinal Chemistry Letters 30(11): e127142. https://doi.org/10.1016/j.bmcl.2020.127142 [PubMed]
- Benítez-Angeles M, Morales-Lázaro SL, Juárez-González E, Rosenbaum T (2020) TRPV1: Structure, endogenous agonists, and mechanisms. International Journal of Molecular Science 21(10): e3421. https://doi.org/10.3390/ijms21103421 [PubMed] [PMC]
- Beskhmelnitsyna EA, Korokin MV, Avtina TV, Martynova OV, Varavin II, Tishin AN (2015) Ion channel TRPA1 is a promising therapeutic target for treatment of pain. Research Results in Pharmacology 1(1): 20–22. https://doi.org/10.18413/2500-235X-2015-1-4-21-24
- Bousquet J, Czarlewski W, Zuberbier T, Mullol J, Blain H, Cristol JP, De La Torre R, Pizarro Lozano N, Le Moing V, Bedbrook A, Agache I, Akdis CA, Canonica GW, Cruz AA, Fiocchi A, Fonseca JA, Fonseca S, Gemicioğlu B, Haahtela T, Iaccarino G, Ivancevich JC, Jutel M, Klimek L, Kraxner H, Kuna P, Larenas-Linnemann DE, Martineau A, Melén E, Okamoto Y, Papadopoulos NG, Pfaar O, Regateiro FS, Reynes J, Rolland Y, Rouadi PW, Samolinski B, Sheikh A, Toppila-Salmi S, Valiulis A, Choi HJ, Kim HJ, Anto JM (2021) Potential interplay between NRF2, TRPA1, and TRPV1 in nutrients for the control of Covid-19. International Archives in Allergy and Immunology 182(4): 324–338. https://doi.org/10.1159/000514204 [PubMed] [PMC]
- Cheng F, Li W, Zhou Y, Shen J, Wu Z, Liu G, Lee PW, Tang Y (2012) AdmetSAR: a comprehensive source and free tool for evaluating chemical ADMET properties. Journal of Chemical Information and Modeling 52(11): 3099–3105. https://doi.org/10.1021/ci300367a [PubMed]
- Daina A, Michielin O, Zoete V (2017) SwissADME: A free web tool to evaluate pharmacokinetics, drug-likeness and medicinal chemistry friendliness of small molecules. Scientific Reports 7(1): e42717. https://doi.org/10.1038/srep42717 [PubMed] [PMC]
- Fernandes ES, Fernandes MA, Keeble JE (2012) The functions of TRPA1 and TRPV1: Moving away from sensory nerves. British Journal of Pharmacology 166(2): 510–521 https://doi.org/10.1111/j.1476-5381.2012.01851.x [PubMed] [PMC]
- Gao Y, Cao E, Julius D, Cheng Y (2016) TRPV1 structures in nanodiscs reveal mechanisms of ligand and lipid action. Nature 534(7607): 347–351. https://doi.org/10.1038/nature17964 [PubMed] [PMC]
- Ghosh M, Schepetkin IA, Özek G, Özek T, Khlebnikov AI, Damron DS, Quinn MT (2020) Essential oils from monarda fistulosa: Chemical composition and activation of transient receptor potential A1 (TRPA1) channels. Molecules 25(21): e4873. https://doi.org/10.3390/molecules25214873 [PubMed] [PMC]
- Hansen KB, Bräuner-Osborne H (2009) FLIPR assays of intracellular calcium in GPCR drug discovery. Methods in Molecular Biology 552: 269–278. https://doi.org/10.1007/978-1-60327-317-6_19 [PubMed]
- Hasan R, Leeson-Payne ATS, Jaggar JH, Zhang X (2017) Calmodulin is responsible for Ca2+-dependent regulation of TRPA1 Channels. Scientific Reports 7: e45098. https://doi.org/10.1038/srep4509 [PubMed] [PMC]
- Humphrey W, Dalke A, Schulten K (1996) VMD: Visual molecular dynamics. Journal of Molecular Graphics 14(1): 33–38. https://doi.org/10.1016/0263-7855(96)00018-5 [PubMed]
- Kamchatnov PR, Evzelman MA, Abusueva BA, Volkov AI (2014) Capsaicin in treatment of neuropathic pain. S.S. Korsakov Journal of Neurology and Psychiatry [Zhurnal Nevrologii i Psikhiatrii im. S.S. Korsakova] 114(11): 135–144. [in Russian]
- Mihai DP, Nitulescu GM, Ion GN, Ciotu CI, Chirita C, Negres S (2019) Computational drug repurposing algorithm targeting TRPA1 calcium channel as a potential therapeutic solution for multiple sclerosis. Pharmaceutics 11(9): e446. https://doi:10.3390/pharmaceutics11090446 [PubMed] [PMC]
- Paulsen CE, Armache J-P, Gao Y, Cheng Y, Julius D (2015) Structure of the TRPA1 ion channel suggests regulatory mechanisms. Nature 520(7548): 511–517. https:// doi.org/10.1038/nature14367 [PubMed] [PMC]
- Trott O, Olson AJ (2010) Autodock Vina: Improving the speed and accuracy of docking with a new scoring function, efficient optimization, and multithreading. Journal of Computational Chemistry 31: 455–461. https://doi.org/10.1002/jcc.21334 [PubMed] [PMC]
- Tseng WC, Pryde DC, Yoger KE, Padilla KM, Antonio BM, Han S, Shanmugasundaram V, Gerlach AC (2018) TRPA1 ankyrin repeat six interacts with a small molecule inhibitor chemotype. Proceedings of National Academy of Science USA 115(48): 12301–12306. https://doi.org/10.1073/pnas.1808142115 [PubMed] [PMC]
- Wang Y, Lin W, Wu N, He X, Wang J, Feng Z, Xie X-Q (2018) An insight into paracetamol and its metabolites using molecular docking and molecular dynamics simulation. Journal of Molecular

Modeling 24(9): e243. https://doi.org/10.1007/s00894-018-3790-9 [PubMed] [PMC]

- Wang YY, Chang RB, Waters HN, McKemy DD, Liman ER (2008) The Nociceptor Ion Channel TRPA1 is potentiated and inactivated by permeating calcium ions. Journal of Biological Chemistry 283(47): 32691–32703. https://doi.org/10.1074/jbc.M803568200 [PubMed] [PMC]
- Xu M, Zhang Y, Wang M, Zhang H, Chen Y, Adcock IM, Chung KF, Mo J, Zhang Y, Li F (2019) TRPV1 and TRPA1 in lung inflammation and airway hyperresponsiveness induced by fine particulate matter (PM2.5). Oxidative Medicine and Cellular Longevity 2019: e7450151. https://doi.org/10.1155/2019/7450151 [PubMed] [PMC]
- Yin S, Zhang L, Ding L et al. (2018) Transient receptor potential ankyrin 1 (TRPA1) mediates il-1β-induced apoptosis in rat chondrocytes via calcium overload and mitochondrial dysfunction. Journal of Inflammation 15: e27. https://doi.org/10.1186/s12950-018-0204-9 [PubMed] [PMC]

Author contributions

- **Aleksey D. Kravchenko**, postgraduate student of the Department of Industrial Pharmacy, e-mail: aleksej_kravchenko97@mail.ru, **ORCID ID** http://orcid.org/0000-0001-6476-0138. The author participated in synthesis of the compounds, was engaged in writing and editing the article.

- **Natalia V. Pyatigorskaya**, Doctor Habil. of Sciences of Pharmacy, Head of the Department of Industrial Pharmacy, e-mail: pyatigorskaya_n_v@staff.sechenov.ru, **ORCID ID** http://orcid.org/0000-0003-4901-4625. The author suggested the idea of the article, made contributions to the design of the article and participated in drafting the article.

- **Galina E. Brkich**, head of the Center for Pharmaceutical Technologies of the Institute of Translational Medicine and Biotechnology, e-mail: brkich@yandex.ru, **ORCID ID** http://orcid.org/0000-0002-3469-9062. The author made contributions to the design of the article and participated in drafting the article.

- **Larysa V. Yevsieieva**, assistant of the Department of Organic Chemistry, e-mail: lar0858@gmail.com, **ORCID ID** http://orcid.org/0000-0002-8427-7036. The author was engaged in writing and editing the article and prepared the final version of the article.

- **Alexander V. Kyrychenko**, Doctor Habil. of Chemical Sciences, Professor at Department of Organic Chemistry e-mail: kyrychen@gmail.com, **ORCID ID** http://orcid.org/0000-0002-6223-0990. The author was engaged in molecular docking calculations, in manuscript writing and editing the final version of the article.

- **Sergiy M. Kovalenko**, Doctor Habil. of Chemical Sciences, Professor of the Department of Organic Chemistry, V.N. Karazin Kharkiv National University, Ukraine; Professor of Department of Pharmaceutical Technology and Pharmacology of the Institute of Pharmacy, I.M. Sechenov First Moscow State Medical University (Sechenov University), e-mail: kovalenko.sergiy.m@gmail.com, **ORCID ID** http://orcid.org/0000-0003-2222-8180. The author was engaged in molecular design and synthesis of the compounds. The author analyzed and interpreted the data, was engaged in writing and editing the article.